Mechanism of Maxi-K Channel Activation by Dehydrosoyasaponin-I

Kathleen M. Giangiacomo,* Augustus Kamassah,‡ Guy Harris,§ and Owen B. McManus‡

From the *Department of Biochemistry, Temple University School of Medicine, Philadelphia, Pennsylvania 19140; and ‡Department of Membrane Biochemistry and Biophysics, and §Department of Natural Products Chemistry, Merck Research Labs, Rahway, New Jersey 07065

ABSTRACT Dehydrosoyasaponin-I (DHS-I) is a potent activator of high-conductance, calcium-activated potassium (maxi-K) channels. Interaction of DHS-I with maxi-K channels from bovine aortic smooth muscle was studied after incorporating single channels into planar lipid bilayers. Nanomolar amounts of intracellular DHS-I caused the appearance of discrete episodes of high channel open probability interrupted by periods of apparently normal activity. Statistical analysis of these periods revealed two clearly separable gating modes that likely reflect binding and unbinding of DHS-I. Kinetic analysis of durations of DHS-I-modified modes suggested DHS-I activates maxi-K channels through a high-order reaction. Average durations of DHS-I-modified modes increased with DHS-I concentration, and distributions of these mode durations contained two or more exponential components. In addition, dose-dependent increases in channel open probability from low initial values were high order with average Hill slopes of 2.4–2.9 under different conditions, suggesting at least three to four DHS-I molecules bind to maximally activate the channel. Changes in membrane potential over a 60-mV range appeared to have little effect on DHS-I binding. DHS-I modified calcium- and voltage-dependent channel gating. 100 nM DHS-I caused a threefold decrease in concentration of calcium required to half maximally open channels. DHS-I shifted the midpoint voltage for channel opening to more hyperpolarized potentials with a maximum shift of −105 mV. 100 nM DHS-I had a larger effect on voltage-dependent compared with calcium-dependent channel gating, suggesting DHS-I may differentiate these gating mechanisms. A model specifying four identical, noninteracting binding sites, where DHS-I binds to open conformations with 10–20-fold higher affinity than to closed conformations, explained changes in voltage-dependent gating and DHS-I-induced modes. This model of channel activation by DHS-I may provide a framework for understanding protein structures underlying maxi-K channel gating, and may provide a basis for understanding ligand activation of other ion channels.

KEY WORDS: calcium-activated potassium channel • potassium channel agonist • ion channel gating • ion channel pharmacology

INTRODUCTION

Ion channels are integral membrane proteins that act as molecular transistors. Binding of a few ligand molecules to the channel or a voltage-dependent conformational change in the channel can lead to large transmembrane ion fluxes driven by electrochemical gradients across the membrane. This process of coupling physiologic stimuli to transmembrane ionic flux is referred to as gating and is an essential feature of ion channel function. Because of this ability to amplify small signals, ion channels are targets of many drugs and toxins.

High conductance calcium-activated potassium (maxi-K)[1] channels are gated open in response to calcium binding to sites located on the intracellular side of the channel, and by depolarized membrane potentials (Marty, 1981; Pallotta et al., 1981; Latorre et al., 1982). A number of scorpion-derived peptides (Miller et al., 1985; Moczydlowski et al., 1988; Galvez et al., 1990) have been found to block maxi-K channels by occluding the extracellular pore (MacKinnon and Miller, 1988; Giangiacomo et al., 1992). Mechanistic studies with these maxi-K channel blockers have revealed structural features of the externally facing mouth of this channel (MacKinnon and Miller, 1989; Park and Miller, 1992*a*, 1992*b*; Knaus et al., 1994; Stampe et al., 1994). Activators of maxi-K channels have been identified from natural (McManus et al., 1993*b*; Singh et al., 1994) and synthetic (Olesen et al., 1994; Hu et al., 1997) sources. By analogy, mechanistic studies of ligands that modulate gating to either block or activate maxi-K channels may provide a means for revealing the structures that underlie gating of these channels.

Dehydrosoyasaponin-I (DHS-I) (Fig. 1) is a triterpene glycoside isolated from *Desmodium adscendens* and is a potent and reversible activator of maxi-K channels (McManus et al., 1993*b*). DHS-I increases open probability of maxi-K channels by acting at a site that is accessible from the intracellular side of the channel (McManus et al., 1993*b*) and may be associated with the β subunit of

Address correspondence to Owen B. McManus, R80-B19, Merck Research Labs, P.O. Box 2000, Rahway, NJ 07065. Fax: 732-594-3925; E-mail: owen_mcmanus@merck.com

[1]*Abbreviations used in this paper:* DHS-I, dehydrosoyasaponin-I; maxi-K channel, high conductance, calcium-activated potassium channel.

this channel (McManus et al., 1995). In this paper, we examine the mechanism of activation of single maxi-K channels from bovine aortic smooth muscle by DHS-I. From this study, we propose a model where binding of four DHS-I molecules maximally activates the maxi-K channel by preferentially binding to the open channel conformation. An abstract of some of these findings has been presented (McManus et al., 1993*a*).

METHODS

Materials

DHS-I was isolated from *Desmodium adscendens* (Sw.) DC. variant *adscendens* (Papillonaceae) as previously described (McManus et al., 1993*b*). DHS-I was dissolved with dimethyl sulfoxide to form a 10-mM stock solution that was stored frozen and remained stable for many months. This concentrated stock solution was diluted with distilled water and dimethyl sulfoxide (90%/10%; vol/vol) to form stock solutions containing 1–1,000 μM DHS-I that were added directly to the bilayer chambers at ~1,000-fold dilution. Final DMSO concentrations were typically <0.01% and had no apparent effects on channel gating at these concentrations. Sarcolemmal membranes were purified from bovine aortic smooth muscle as described previously (Slaughter et al., 1989). 1-Palmitoyl-2-oleoylphosphatidylethanolamine (POPE) and 1-palmitoyl-2-oleoylphosphatidylcholine (POPC) were purchased from Avanti Polar Lipids, Inc. (Birmingham, AL).

Fusion of Maxi-K Channels with Planar Lipid Bilayers

Planar lipid bilayers were formed by applying a solution of POPE and POPC in a 7/3 molar ratio dissolved in decane (50 mg/ml) to an ~200-μm hole in a polycarbonate partition separating two chambers. Bilayers readily formed with capacitances of 150–250 pF. Bovine aortic sacrolemmal membranes were then applied to the *cis* side of the bilayer under an osmotic gradient. After incorporation of a maxi-K channel, the concentration of KCl was raised on the *trans* side, resulting in equivalent concentrations (150 mM) of KCl on both sides of the bilayer for all experiments. The orientation of a fused channel was determined from calcium and voltage dependence of channel gating. Channels typically fused with the intracellular side of the channel facing the *cis* chamber, and 100 μM EGTA was then added to the outside. The pH was buffered to 7.2 with 10 mM HEPES and 3.7 mM KOH. The experimental solutions contained ~0.3 μM calcium as a contaminant, which was determined by atomic absorption spectrophotometry and confirmed using maxi-K channels as biosensors. This amount of contaminant calcium was included in calculations of total calcium for the experiments measuring calcium-dependent changes in channel gating. Experiments were done at 23–25°C.

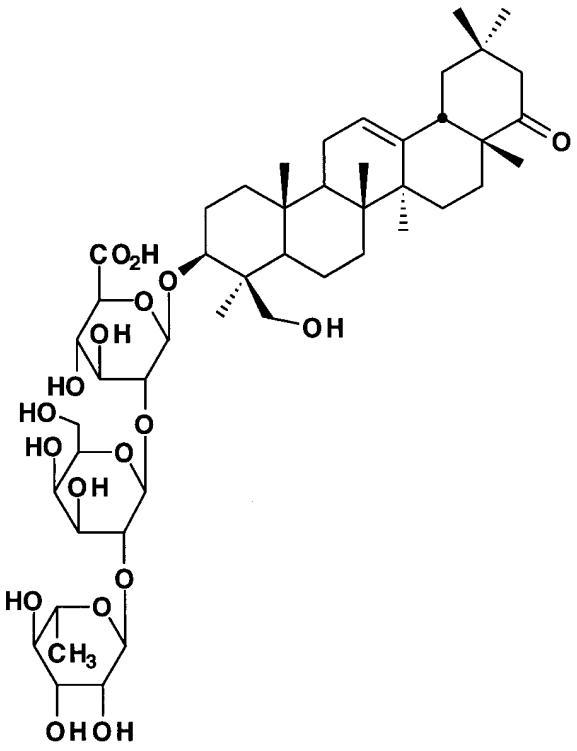

FIGURE 1. Structure of dehydrosoyasaponin-I.

Recording and Analysis of Single-Channel Currents

Currents flowing across the bilayer were recorded with standard electrophysiological methods. The inputs to the amplifiers were connected to the experimental chambers with Ag/AgCl wires via agar bridges containing 0.2 M KCl. The external side of the channel was defined as 0 mV and currents flowing from the internal to external side are represented as positive currents. Currents were recorded on video tape after digital encoding with a VR-10 digital recorder (Instrutech Corp., Elmont, NY). Before analysis, the single channel currents were filtered with an eight-pole Bessel filter (4302, pulse mode; Ithaco, Ithaca, NY) so that noise peaks were clearly less than half the current amplitude of an open channel. Additional filtering was sometimes applied using a digital Gaussian filter implemented in the TAC program.

Single channel currents were analyzed on a DEC 11/73 computer (Digital Equipment Corp., Maynard, MA) after digitization with a DT2782-8D1A analogue to digital converter (Data Translation Corp., Marlboro, MA) or on Macintosh computers after digitization with an ITC-16 interface (Instrutech Corp.) and idealization using Acquire and TAC programs (Bruxton Corp., Seattle, WA). The durations of channel open and closed times were determined by measuring the sequence of times between crossings of a threshold set halfway between open and closed current amplitudes. Distributions of event durations were plotted and fit with sums of exponential components using maximum likelihood methods as previously described (McManus et al., 1987) or using TACFIT (Bruxton Corp.). Single channel open probability was fit with Hill and Boltzmann equations (see text) by minimizing chi squared differences. Error bars represent SEM.

Analysis of DHS-I-modified and Normal Gating Modes

A kinetic analysis of DHS-I-induced modes was performed on single maxi-K channels that displayed stable gating behavior in the absence of DHS-I. Gating of four single channels was analyzed in detail, each of which exhibited primarily a single mode of gating activity during 20–40 min of control recording. To identify changes in gating, we plotted running averages of small groups of consecutive open- and closed-interval durations. For each experiment, we empirically determined the optimal number of events to average, which was typically between 5 and 10 open and closed event pairs. The ideal number of events for averaging is large enough to minimize the stochastic variation in event durations for each gating mode and brief enough to allow faithful resolution of the transition times between modes. Channel open probability in the absence of DHS-I was adjusted with calcium or membrane potential to fall between 0.01 and 0.15. At this level of

activity, DHS-I caused large changes in mean open and closed times that were easily detected, and control openings occurred at a rate that was equal to or faster than the apparent rate of interaction of DHS-I with a single channel. The methods and criteria used for separation of DHS-I-induced gating modes are described in detail in the RESULTS and in Table I. Durations of periods in a gating mode were calculated from summed times between excursions across these criteria, in much the same way that threshold detection is used to calculate open and closed times from a digitized record. The durations of normal and DHS-I-modified gating modes were fit with kinetic schemes using maximum likelihood and Q-matrix methods as previously described (McManus and Magleby, 1991). Corrections for missed events were not applied.

RESULTS

Fig. 2 illustrates how DHS-I (Fig. 1) modifies gating of a single maxi-K channel. In control, channel open probability was low (0.04) and brief bursts of channel openings are separated by much longer closed periods lasting about a second. Addition of 33 nM DHS-I to the intracellular side of the channel caused a clear increase in average channel open probability to 0.45, and 67 nM DHS-I caused a further increase in channel open probability to 0.75. Inspection of the single channel record suggests a possible mechanism for activation of the channel by DHS-I. A striking difference from control is the appearance of discrete episodes of high channel open probability in the presence of DHS-I. These spurts of elevated channel open probability can be clearly seen on a slow time scale in Fig. 2 *A*, and are separated by periods of channel activity apparently similar to control gating. A simple explanation of this effect is that the spurts of elevated channel open probability represent times when DHS-I is bound to the channel. The periods of elevated channel open probability appear longer at 67 than at 33 nM DHS-I, suggesting that more than one DHS-I molecule can bind to a maxi-K channel and affect channel gating. For a bimolecular process, durations of periods of drug-modified activity should remain independent of drug concentration, while frequency of occurrence of these episodes should increase with drug concentration. Since the durations of drug-modified episodes appear to increase with DHS-I concentration, DHS-I may activate maxi-K channels by acting at multiple sites on the intracellular side of the channel.

Concentration Dependence of Activation of Maxi-K Channels by DHS-I

Inspection of the single channel currents in Fig. 2 suggests that DHS-I binds to multiple functional sites on maxi-K channels. We quantitatively examined the stoichiometry of this interaction by measuring the relation between channel open probability and DHS-I concentration. In Fig. 3 *A*, open probability of a single maxi-K channel is plotted against DHS-I concentration on log–log axes. In the absence of DHS-I, channel open probability was low (0.0035). Adding DHS-I to the internal side caused a steep increase in channel open probability to nearly one at higher concentrations. Channel open probability was well-described by a modified Hill equation:

$$P_o = P_{o(\min)} + \frac{(1 - P_{o(\min)}) * [\mathrm{DHS}]^{N_{\mathrm{DHS}}}}{[\mathrm{DHS}]^{N_{\mathrm{DHS}}} + (K_{\mathrm{DHS}})^{N_{\mathrm{DHS}}}} \qquad (1)$$

where $P_{o(\min)}$ is the channel open probability observed in the absence of DHS-I, K_{DHS} is the concentration of DHS-I that caused a half-maximal increase in channel open probability, and N_{DHS} is the Hill coefficient. The Hill coefficient for this experiment was 3.4, and the mean value of five experiments done under the same conditions was 2.4 ± 0.34, suggesting that binding of approximately four or more DHS-I molecules to the channel may be required, under these conditions, for maximal activation. The range of Hill coefficients we observed for DHS-I activation, from 1.5 to 3.4, is similar to the Hill coefficients previously observed for calcium activation of these channels (Giangiacomo et al., 1995).

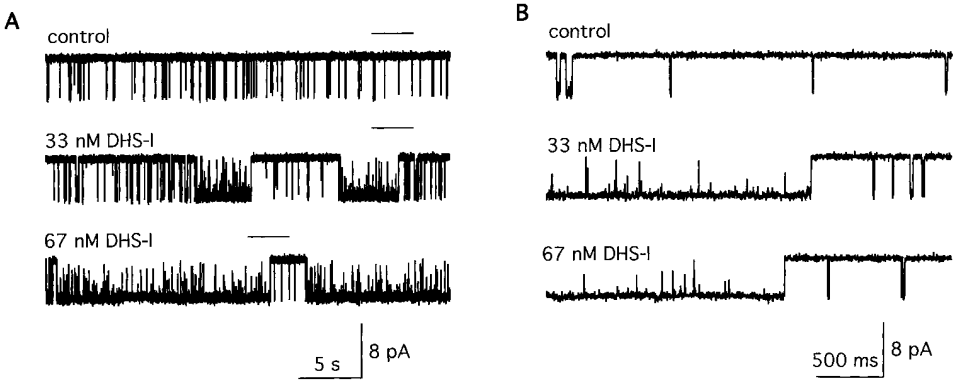

FIGURE 2. DHS-I activation of a single maxi-K channel incorporated into a planar lipid bilayer. Currents through a single channel in the presence of 0, 33, and 67 nM DHS-I on the internal side are shown on a slow (*A*) and faster (*B*) time scale. The solid lines above the data in *A* indicate periods that are expanded in *B*. Channel opening produces downward current deflections. Currents were filtered at 200 Hz. Both sides of the bilayer contained 150 mM KCl, 10 mM HEPES, 3.7 mM KOH, 5 μM $CaCl_2$, pH 7.2, and the membrane potential was held at −20 mV.

The K_{DHS} value for the experiment shown in Fig. 3 *A* was 60 nM, and the average value of five experiments done under conditions of +30 mV and 2 μM calcium was 170 ± 79 nM. The K_{DHS} values obtained varied over approximately an eightfold range in these experiments. The experiment shown in Fig. 3 *A* was among the more sensitive to DHS-I activation, but was not unusual; K_{DHS} values calculated for three of the five experiments were between 60 and 70 nm. A similar range of sensitivity to calcium-dependent activation was observed for these channels, with a membrane potential of −30 mV (Fig. 4), and for maxi-K channels from skeletal muscle (McManus and Magleby, 1991). Some channels (~10–20%) appear less sensitive to activation by calcium and DHS-I, which affects the average values. The absolute values of K_{DHS} measured in these experiments are simply empirical measures of the sensitivity of channel gating to DHS-I under certain conditions, and cannot be directly related to the affinity of DHS-I binding to sites on the channel. This occurs because of the unknown relation between occupancy of DHS-I binding sites on the channel and channel open probability.

These data tell us two simple facts about the mechanism of channel activation by DHS-I. First, a single maxi-K channel must have four or more functionally relevant DHS-I binding sites. Second, starting from low channel open probabilities in the absence of DHS-I, maxi-K channels can be maximally activated by high concentrations of DHS-I. High concentrations (>1 μM) of DHS-I were applied in four experiments done at 2 μM Ca and +30 mV, and the average maximum open probability was 0.97. Thus, in the presence of low concentrations of calcium at +30 mV, DHS-I causes large increases in the open probability and hence the effective equilibrium for channel opening.

Voltage Dependence of DHS-I Binding

Are the effects of DHS-I on maxi-K channel gating dependent on the membrane potential? DHS-I contains a carboxylate group on a glucuronic acid that can have a negative charge at neutral pH. If this part of the molecule senses the membrane field when bound to the channel, then membrane potential might exert an effect on DHS-I binding to the channel. To address this question, we examined the concentration-dependent effects of DHS-I on open probability at two different voltages.

The DHS-I binding reaction and membrane potential both influence the equilibrium for channel opening. To keep the equilibrium for channel opening constant at the two membrane potentials, we used intracellular calcium to maintain similar control open probabilities. The experiments described above were done at +30 mV and 2 μM calcium. We also did similar

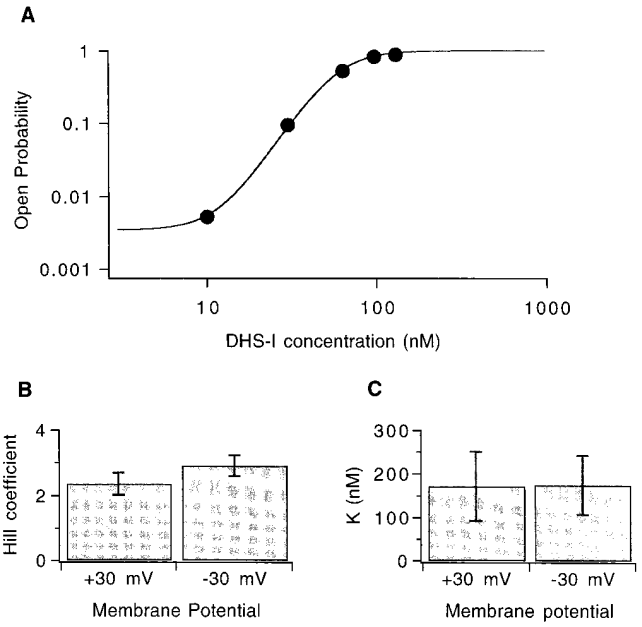

FIGURE 3. Concentration-dependent effects of DHS-I on single channel open probability. (*A*) Open probability from a single channel is plotted as a function of DHS-I concentration at the inside when the membrane potential was +30 mV and intracellular calcium was 2 μM. The solid line represents the best fit of the data to a modified Hill equation (Eq. 1) with a K_{DHS} value of 60 nM and a Hill slope (N_{DHS}) of 3.4. (*B*) Average Hill slopes obtained from plots of P_o versus DHS-I from several experiments are plotted at +30 ($n = 5$) and −30 mV ($n = 5$). Intracellular calcium was 2 μM at +30 mV and 5 μM at −30 mV. (*C*) Average K_{DHS} values from the same experiments as in *B* are plotted at +30 and −30 mV.

experiments at −30 mV, but increased the internal calcium concentration to 5 μM so that the control open probabilities were similar (0.0042 ± 0.0031 at −30 mV and 0.0091 ± 0.0039 at +30 mV). Fig. 3 *C* shows that the K_{DHS} values for DHS-I averaged from several experiments were similar at +30 mV and at −30 mV, (170 ± 79 and 170 ± 67 nM, respectively). In addition, the average Hill coefficient values from these experiments were similar, 2.9 ± 0.3 at −30 mV compared with 2.4 ± 0.3 at +30 mV, Fig. 3 *B*. These results reveal that the concentration-dependent effects of DHS-I on open probability are not modified by a 60-mV change in membrane potential. Consequently, the DHS-I binding reaction itself is not voltage dependent.

DHS-I Shifts Calcium-dependent Channel Gating to Lower Concentrations

Activation by intracellular calcium is a defining feature of maxi-K channels. DHS-I does not substitute for calcium in causing channel opening at membrane potentials where channel opening requires calcium (McManus et al., 1993*b*). However, it may modify the ability of calcium to open maxi-K channels. The effects of

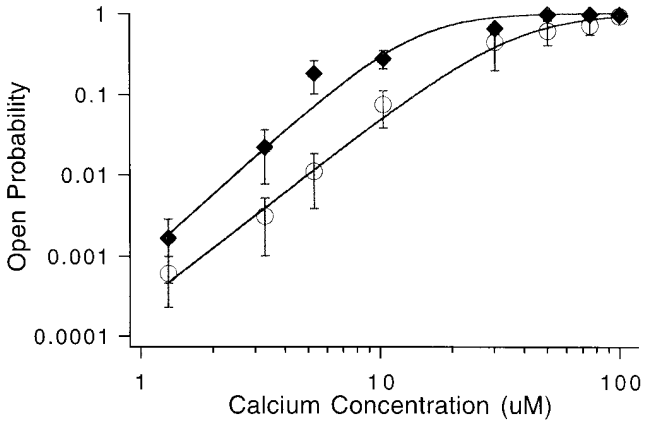

FIGURE 4. Effects of DHS-I on calcium-dependent channel gating. Average open probability of single maxi-K channels from several experiments was measured as a function of calcium concentration in the absence (○) and presence (◆) of 100 nM DHS-I. Solid lines represent fits to the data using a Hill equation of the form $P_o = 1/(1 + K_{Ca}^{N_{Ca}}/[Ca]^{N_{Ca}})$. Membrane potential was −30 mV.

DHS-I on calcium-dependent channel opening are shown in Fig. 4 for channels held at −30 mV. 100 nM DHS-I shifted the midpoint of the channel open probability–calcium relation by about threefold. When a Hill equation for calcium was fit to averaged data from many experiments (Fig. 4), the K_{Ca} value decreased from 37 μM in control to 14 μM in the presence of 100 nM DHS-I. The Hill slope (N_{Ca}), which gives an estimate of the minimum number of calcium ions involved in channel opening, increased slightly from 2.3 to 2.6 after addition of 100 nM DHS-I. When data from individual experiments were fit separately, the K_{Ca} values (38 ± 14 μM in control and 13 ± 2 μM with 100 nM DHS-I; $P < 0.05$) were similar to the values obtained from fitting the average values. The Hill slopes calculated for individual experiments were not significantly different in DHS-I (3.2 ± 0.4) compared with control (2.8 ± 0.2). Hill slopes obtained from fitting average P_o values versus DHS-I concentration were lower than the average Hill slope obtained from fitting individual experiments due to variations in K_{Ca} values between channels. Nevertheless, 100 nM DHS-I had little effect on the Hill slope obtained with either method. The effects of DHS-I on channel open probability were smaller at low calcium (1.3 μM) than those observed at higher calcium concentrations (5 μM). Indeed, in some cases the effects of DHS-I on channel opening at 1.3 μM calcium were almost negligible. This is consistent with previous observations that DHS-I may require the presence of calcium to stimulate channel opening (McManus et al., 1993*b*). DHS-I caused an increase in the sensitivity of channel gating to calcium, but had little apparent effect on the minimum number of calcium ions required for full channel opening.

DHS-I Shifts Voltage-dependent Channel Gating to More Negative Potentials

We next asked whether voltage-dependent maxi-K channel gating was affected by DHS-I. Fig. 5 *A* shows the relation between open probability of a single maxi-K channel and membrane potential (V_m), which can be described by a Boltzmann equation (*solid line*). The slope of this line tells us that channel open probability increased e-fold per 10.0 mV and the midpoint for channel activation ($V_{1/2}$) was 27.7 mV in the absence of DHS-I. In the presence of 10 nM DHS-I, this channel opened at more negative potentials than in control. The midpoint for channel activation was shifted by 17.3 mV to more negative potentials, while the slope of the curve decreased slightly to e-fold per 12.3 mV. This effect of DHS-I on voltage-dependent channel activation is similar, in this case, to the effects of intracellular calcium.

Increasing the concentration of DHS-I led to larger shifts in the midpoint for channel opening. Fig. 5 *B* shows the quantitative relationship between the absolute shift in $V_{1/2}$ ($\Delta V_{1/2}$) and the concentration of DHS-I, averaged from twelve similar experiments. As the concentration of DHS-I was raised, the hyperpolarizing shift in $V_{1/2}$ increased and appeared to saturate near 100 mV. That is, at very negative potentials, the channel will not open, even in the presence of saturating concentrations of DHS-I. This result suggests that there is a voltage-dependent step in the gating process that occurs after binding of DHS-I to the channel. This saturation is consistent with the idea that DHS-I binds to a limited number of specific binding sites on the channel. Fig. 5 *C* plots the corresponding slopes of voltage-dependent channel opening as a function of DHS-I concentration. No clear change in the slope of the voltage dependence of channel activation was observed as the concentration of DHS-I was raised. In addition, we examined the relationships between mean open and closed times versus membrane potential. The slopes of these curves in the absence and presence of DHS-I were similar (not shown). Thus, DHS-I increases the equilibrium for channel opening without effecting the slopes of voltage-gating functions.

The effects of DHS-I on voltage-dependent gating require preferential binding of DHS-I to open states. To understand these effects of DHS-I binding, we examined a greatly simplified model of maxi-K channel gating, shown in Scheme I, in which, in the absence of DHS-I, there are two sets of states, closed (C) and open (O). The transition between these states, and consequently the effective equilibrium for channel opening, K_{eq}, is voltage dependent. DHS-I binds to both closed and open states, but it binds more tightly when the channel is open. Furthermore, high order effects of DHS-I on channel open probability, (see Figs. 2 and 3)

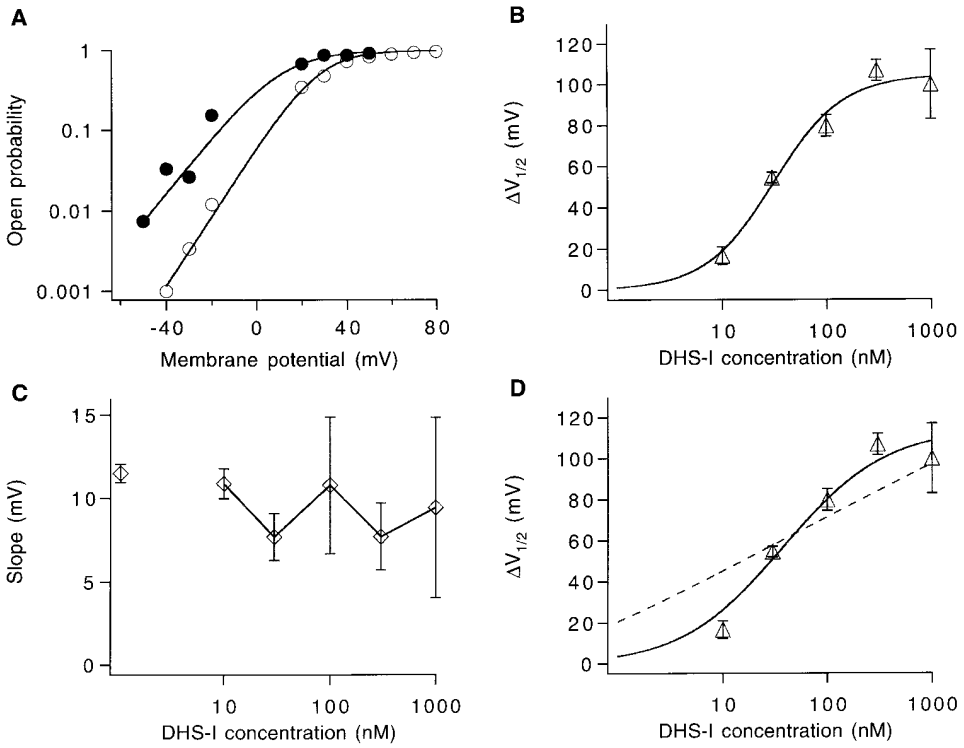

FIGURE 5. Effects of DHS-I on voltage-dependent channel gating. (*A*) Open probability from a single channel is plotted as a function of voltage with zero (○) and 10 (●) nM DHS-I at the inside. The solid lines represent the best fit of the data to the Boltzmann equation $P_o = 1/\{1 + \exp[(V_{1/2} - V_m)/s]\}$ (see text for explanation of variables). (*B*) The shift in $V_{1/2}$, averaged from several experiments, is plotted as a function of concentration of DHS-I. $V_{1/2}$ values were obtained from fitting plots of open probability versus membrane potential to a Boltzmann equation for each experiment. The line represents the best fit of the data to a Hill equation of the form

$$\Delta V_{1/2} = \Delta V_{1/2\,(max)} / (1 + K_{DHS}^{N_{DHS}} / [\text{DHS-I}]^{N_{DHS}}),$$

with a K_{DHS} value of 31 nM, a slope (N_{DHS}) of 1.3, and a maximum shift in $V_{1/2}$ ($\Delta V_{1/2(max)}$) of 105 mV. (*C*) Slopes of voltage dependence of channel activation are plotted as a function of DHS-I concentration. These *s* values were obtained from fits of single channel open probability versus membrane potential to a Boltzmann equation for each experiment from the same set of experiments described in *B*. The far left point represents values obtained in the absence of DHS-I. (*D*) A model for DHS-I activation describes the observed hyperpolarizing shift in $V_{1/2}$. The observed shift in $V_{1/2}$, from *B*, is plotted as a function of DHS-I concentration. The solid line represents the best fit of the data to Eq. 7 (least squares minimization) where the model includes four identical, independent DHS-I binding sites. The k_c and k_o values obtained from this fit were 130 and 11 nM, respectively, while the maximum predicted shift in $V_{1/2}$ was 107 mV. The dashed line represents the best fit of the data to the same model with only one DHS-I binding site. Intracellular $CaCl_2$ was 10 μM.

suggest a minimum of three to four DHS-I binding sites on the maxi-K channel.

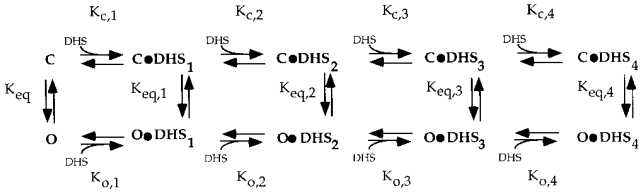

(SCHEME I)

We first asked whether this model could describe the effects of DHS-I on voltage-dependent gating of the maxi-K channel. In particular, we asked whether the model shown in Scheme I can quantitatively describe the hyperpolarizing shift in $V_{1/2}$ caused by DHS-I, as shown in Fig. 5 *B*. To do this, we first expressed Scheme I in terms of open probability, P_o, using the equation,

$$P_o = \left[1 + \frac{c + c \bullet DHS_1 + c \bullet DHS_2 + c \bullet DHS_3 + c \bullet DHS_4}{o + o \bullet DHS_1 + o \bullet DHS_2 + o \bullet DHS_3 + o \bullet DHS_4}\right]^{-1}, \quad (2)$$

where c, c • DHS_1, c • DHS_2, c • DHS_3, and c • DHS_4 represent occupancies of channel closed states with 0, 1, 2, 3, and 4 DHS-I molecules bound, respectively. And, o, o • DHS_1, o• DHS_2, o • DHS_3, and o • DHS_4 represent occupancies of open states with 0, 1, 2, 3, and 4 DHS-I molecules bound, respectively. Eq. 2 can be described in terms of the macroscopic equilibrium dissociation constants for DHS-I binding to closed and open states,

$$P_O = \left[1 + \frac{c}{o}\left(\frac{1 + \frac{[DHS]}{K_{c,1}} + \frac{[DHS]^2}{K_{c,1}K_{c,2}} + \frac{[DHS]^3}{K_{c,1}K_{c,2}K_{c,3}} + \frac{[DHS]^4}{K_{c,1}K_{c,2}K_{c,3}K_{c,4}}}{1 + \frac{[DHS]}{K_{o,1}} + \frac{[DHS]^2}{K_{o,1}K_{o,2}} + \frac{[DHS]^3}{K_{o,1}K_{o,2}K_{o,3}} + \frac{[DHS]^4}{K_{o,1}K_{o,2}K_{o,3}K_{o,4}}}\right)\right]^{-1}, \quad (3)$$

where $K_{o,1}$, $K_{o,2}$, $K_{o,3}$, and $K_{o,4}$ represent the macroscopic equilibrium dissociation constants for binding of 1, 2, 3, and 4 DHS-I molecules to open states. Simi-

larly, the macroscopic equilibrium dissociation constants for binding of 1, 2, 3, and 4 DHS-I molecules to closed states are described by $K_{c,1}$, $K_{c,2}$, $K_{c,3}$, and $K_{c,4}$, respectively. When the sites are identical and noninteracting, it can be shown that Eq. 3 simplifies to:

$$P_o = \left[1 + \left(\frac{c}{o}\right) * \left(\frac{\left(1 + \frac{[DHS]}{k_c}\right)^n}{\left(1 + \frac{[DHS]}{k_o}\right)^n}\right)\right]^{-1}, \quad (4)$$

where k_c and k_o represent the microscopic equilibrium dissociation constants for DHS-I binding to the closed and open states, respectively, and n represents the number of DHS-I binding sites. The effect of voltage on the equilibrium for channel opening in the absence of DHS-I can be described by a Boltzmann equation,

$$\frac{c}{o} = \frac{1}{K_{eq}} = \exp\left(\frac{V_{1/2} - V_m}{s}\right), \quad (5)$$

where V_m represents the membrane potential, $V_{1/2}$ represents the voltage at which the channel is half-maximally activated, and s describes the slope in mV. Substituting Eq. 5 into 4 yields Eq. 6, which describes the effects of DHS-I on the voltage dependence of maxi-K channel open probability:

$$P_o = \left[1 + \left(\exp\frac{V_{1/2} - V_m}{s}\right) * \left(\frac{\left(1 + \frac{[DHS]}{k_c}\right)^n}{\left(1 + \frac{[DHS]}{k_o}\right)^n}\right)\right]^{-1}. \quad (6)$$

To test whether this model can quantitatively describe the hyperpolarizing shift in $V_{1/2}$ caused by DHS-I, the P_o in Eq. 6 was set to 0.5. This is a reasonable assumption since, under the conditions of these experiments, P_o was 0.5 at $V_{1/2}$. Including these terms and rearranging Eq. 6 yields Eq. 7, which can be used to fit the data to the model shown in Scheme I:

$$\Delta V_{1/2} = s * \ln\left(\frac{\left(1 + \frac{[DHS]}{k_o}\right)^n}{\left(1 + \frac{[DHS]}{k_c}\right)^n}\right). \quad (7)$$

Fig. 5 *D* shows results of fitting Eq. 7 to the quantitative relationship between $\Delta V_{1/2}$ and concentration of DHS-I, averaged from twelve similar experiments. In these fits, the slope s of voltage-dependent gating was constrained to the average value (11.5 mV) measured from twelve different experiments in the absence of DHS-I. The microscopic equilibrium dissociation constants for DHS-I binding to closed and open states, k_c and k_o, respectively, were allowed to vary. When data were fit to the four-site model (Fig. 5 *D, solid line*) by minimizing least-squared differences, a unique solution was obtained where k_c for DHS-I binding to closed states of the channel was 130 nM and k_o for DHS-I binding to open states of the channel was 11 nM. A one-site model for DHS-I binding did not adequately describe the data (Fig. 5 *D, dashed line*). Surprisingly, a simple model with four independent DHS-I binding sites, where DHS-I exhibits a 12-fold higher binding affinity for open states relative to closed states, provides an excellent description of the hyperpolarizing shift in $V_{1/2}$.

The model in Scheme I also makes a prediction about the relationship between single-channel open probability and concentration of DHS-I. At very negative membrane potentials, where the equilibrium for channel opening in the absence of DHS-I is very low, maximum open probability in the presence of DHS-I is not predicted to reach 1. Rather, it is predicted to saturate at values <1 at negative membrane potentials. This occurs because effects of DHS-I on channel opening are limited by the relative affinities of DHS-I for closed and open states and by saturability of the binding reaction. Thus, the favorable shift in equilibrium for channel opening, K_{eq}, caused by DHS-I binding is finite. As membrane potential is hyperpolarized, the unfavorable shift in K_{eq} induced by voltage cannot be overcome by favorable effects of DHS-I on channel opening.

To test this prediction of the model, we examined the concentration-dependent effects of DHS-I on single channel open probability at −70 mV, which is 104 mV more negative than the $V_{1/2}$ observed in the absence of DHS-I (34.5 ± 4.6 mV) with 10 μM calcium. This difference in holding potential matches the maximum observed shift in $V_{1/2}$ observed after treatment with 1,000 nM DHS-I. Fig. 6 *A* shows data from a single experiment and Fig. 6 *B* plots open probability versus DHS-I averaged from five experiments. The solid line in Fig. 6 *B* represents the model, as described by Eq. 6, using parameters solely determined from fitting the model to data shown in Fig. 5 *D*. The data are well described by this model and, as predicted, the concentration-dependent increase in channel open probability caused by DHS-I saturates at a value <1. Thus, at this gross level, the model shown in Scheme I explains the observed effects of DHS-I on voltage-dependent channel gating.

Analysis of DHS-I-induced Gating Modes

The effects of DHS-I on voltage-dependent channel opening can be explained by high order preferential binding of DHS-I to open states. To understand this preferential binding mechanistically, we examined the kinetic pattern of channel gating caused by DHS-I (shown in Fig. 2). In the presence of DHS-I, bursts of high channel open probability are separated by periods of lower open probability that appear similar to control. These periods of high open probability may represent periods when DHS-I is bound to the channel. As expected for high-order binding, durations of these pe-

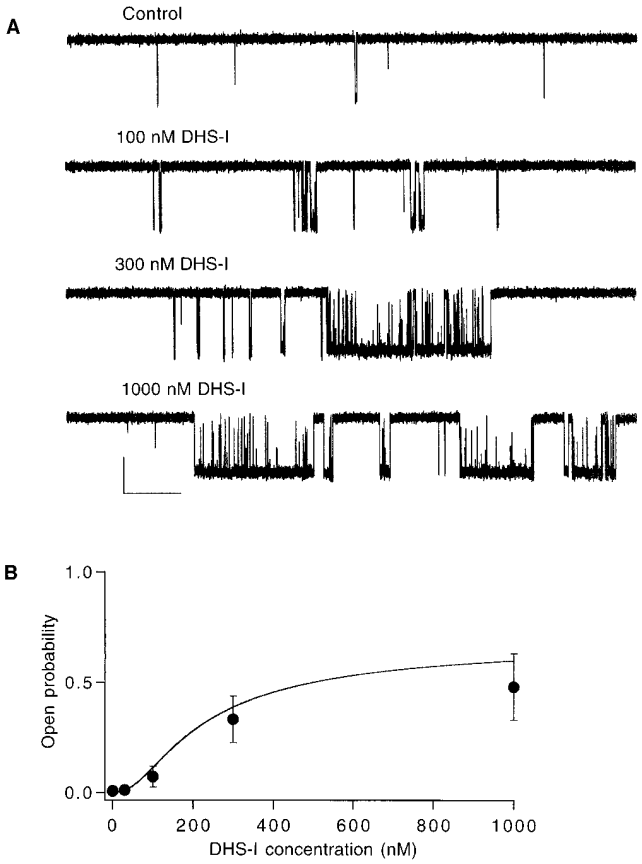

FIGURE 6. A prediction of the four-independent, noninteracting site model. The effects of DHS-I on single channel open probability saturate at values <1 at a negative membrane potential. (*A*) Currents through a single maxi-K channel are shown with 0, 100, 300, and 1,000 nM DHS-I at the inside when the membrane potential was −70 mV and intracellular calcium was 10 μM. (*B*) Single channel open probability, averaged from several different experiments, is plotted as a function of the concentration of DHS-I. The solid line describes the model for DHS-I activation in terms of single channel open probability (Eq. 6). Values for the parameters, k_c and k_o, were obtained from a fit of the model to data shown in Fig. 5. The current scale is 10 pA and the time scale is 500 ms.

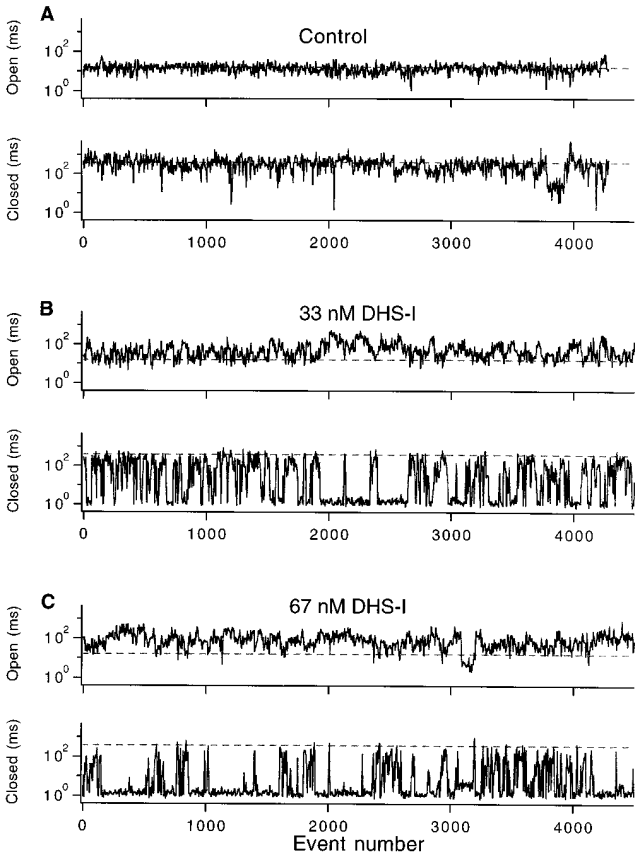

FIGURE 7. Stability plots of mean open and closed times. Average durations of five sequential open or closed times are plotted in control (*A*), and in the presence of 33 nM DHS-I (*B*) and 67 nM DHS-I (*C*). All 8,599 open and closed events recorded during a 28.7-min control period are shown. A similar number of events is displayed for each DHS-I concentration. Note that the x axis is not a linear time scale. Mean open and closed times from control are plotted as dashed lines. The changes in channel gating caused by DHS-I in this experiment led to an increase in channel open probability from 0.0393 in control to 0.423 in 33 nM DHS-I, and 0.749 in 67 nM DHS-I. Currents were filtered at 400 Hz, membrane potential was −20 mV, with 5 μM calcium.

riods of high P_o appeared to increase with increasing concentrations of DHS-I. Conversely, the periods of low open probability may represent when DHS-I is not bound to the channel. To examine this hypothesis, we performed a kinetic analysis of bursts of openings associated with DHS-I interaction with single maxi-K channels.

A kinetic analysis of bursts of high channel open probability requires that we identify periods of normal and modified channel gating. As a first step, we chronologically calculated mean open and closed times for groups of sequential intervals. Fig. 7 shows stability plots that display changes in mean open and closed times in the absence, and presence, of DHS-I. In control, mean open and closed times were stable over time, and were each primarily limited to a single level. Stability plots reveal a striking effect of DHS-I on channel gating. In the presence of DHS-I, mean closed times alternated between two distinct levels separated by approximately two log units. One level was similar to mean closed times measured in control (Fig. 7, *dashed lines*) and the other level was much briefer. In addition, DHS-I increased the variability of mean open times and caused a shift to higher mean open times, but distinct levels were not identified. Scatter plots (Fig. 8, *A–C*) of this data use both mean open and mean closed times for segregating data. These scatter plots reveal two types of gating activity in the presence of DHS-I and one type of gating activity in control. Distributions of mean open and closed times (Fig. 8, *D* and *E*) provide a quantitative view of data shown in the scatter plots and reaffirm the idea that control kinetic data are con-

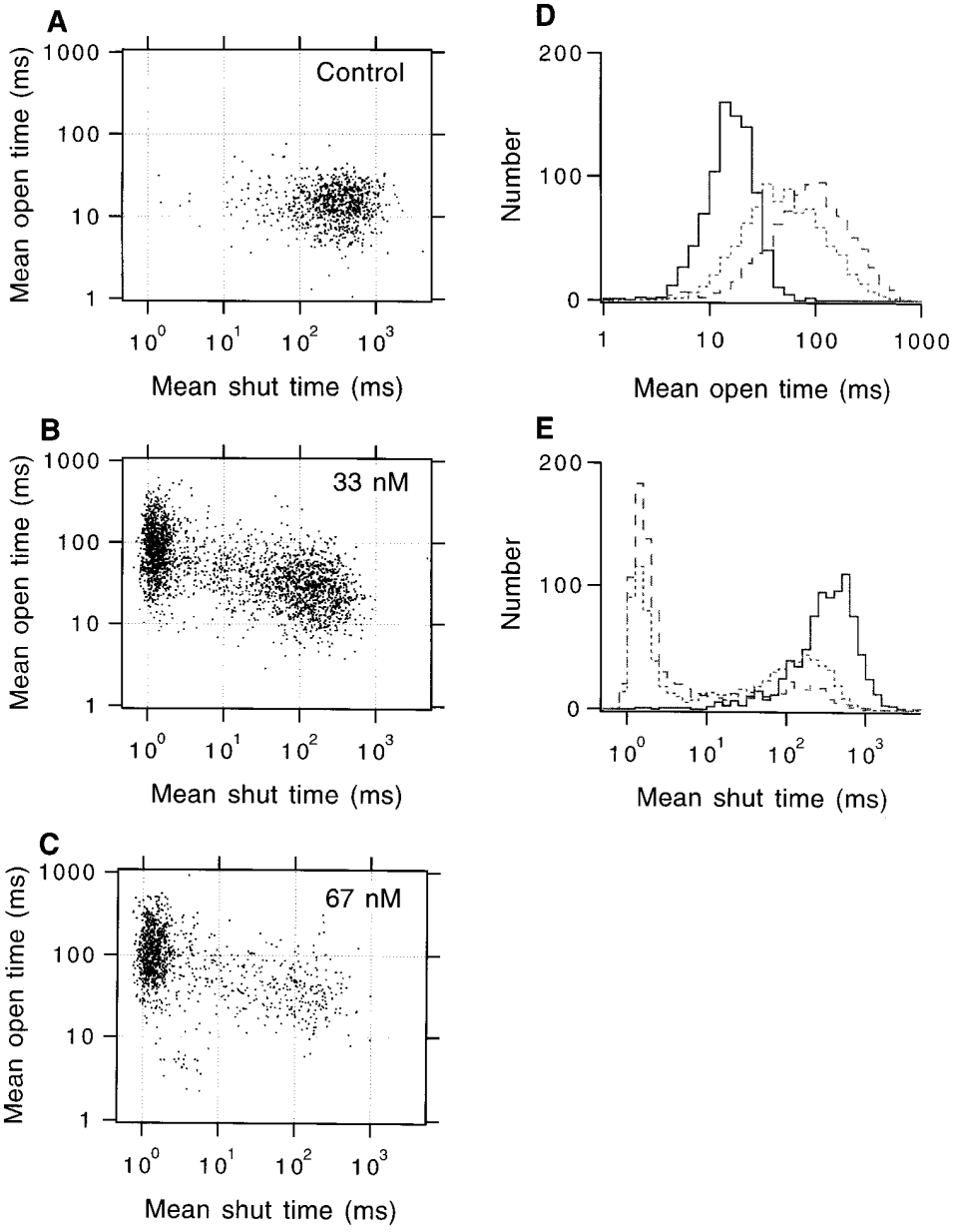

FIGURE 8. Characterization of gating shifts caused by DHS-I. Mean open and closed times were calculated for groups of five sequential pairs of open and closed times and plotted against each other for control data (*A*), and for data recorded in the presence of 33 nM DHS-I (*B*) and 67 nM DHS-I (*C*). Logarithmic histograms of mean open and closed times are shown in *D* and *E*, respectively. The solid lines in *D* and *E* plot distributions of mean open and closed times from control, and the dotted and dashed lines represent mean open and closed times recorded in 33 and 67 nM DHS-I, respectively. Data are from the same experiment shown in Fig. 7. A total of 24,389 events were recorded (31.4 min) with 33 nM DHS-I, and 11,386 events were recorded (13.5 min) with 67 nM DHS-I.

tained within a single population, while two types of gating behavior are seen in the presence of DHS-I.

The two patterns of gating activity seen in the presence of DHS-I may represent periods of drug-modified gating and periods of normal activity. Transitions between these patterns of gating were abrupt. This is consistent with the proposal that these patterns of activity reflect DHS-I binding events. The high open probability mode corresponding to a DHS-I:channel complex was characterized by brief closed and long open times. Mean open and mean closed times from the lower open probability mode were similar to control. This gating pattern in the presence of drug reminds of modal gating of calcium channels caused by dihydropyridine agonists (Hess et al., 1984), so we adopted this terminology. The two gating modes seen in the presence of DHS-I were separated by criteria derived from an examination of plots of mean open and closed times (Fig. 8). For the experiment shown in Fig. 8, drug-modified groups of events were defined as groups with a mean closed time <10 ms or mean open time >200 ms. Using these criteria, nearly all control events were categorized as normal mode (fractional occupancy was 0.9996). Increasing the concentration of DHS-I from 33 to 67 nM caused a decrease in fraction of time spent in the normal mode from 0.685 to 0.318 and an increase in duration and frequency of drug-modified periods.

How do the shifts in channel gating seen in the pres-

ence of DHS-I relate to occupancy of the channel by different numbers of DHS-I molecules? If channel gating can respond equally to binding of four DHS-I molecules, then we might expect to observe five gating modes corresponding to occupancy of zero to four DHS-I molecules. However, we detected only two distinct modes in the presence of DHS-I. One framework for interpreting these results proposes that normal mode gating in the presence of DHS-I occurs with no DHS-I molecules bound, and modified gating occurs with one to four molecules bound. This proposal predicts identity between control gating and normal mode gating in the presence of DHS-I. Examination of Fig. 8 shows that these two populations of events differ slightly; closed times were longer and open times were briefer in control compared with normal mode events seen in DHS-I. This small shift may be due to inclusion of a few drug-modified events in groups that were primarily composed of normal mode events. This would occur at transitions between two gating modes. Alternatively, normal mode events seen in the presence of DHS-I might reflect occupancy by zero to one or more DHS-I molecules. Why do we see only a single modified mode in the presence of DHS-I if one to four DHS-I molecules can be bound during a modified mode? Part of the answer comes from the fact that channel open probability cannot exceed one, which limits an ability to detect increases in channel open probability. The channel open probability in modified periods from data shown in Figs. 7 and 8 was 0.98 at both DHS-I concentrations. In addition, it may be difficult to detect modes that are infrequently represented. A kinetic analysis of the mode durations can provide additional information about the number of DHS-I molecules bound during the different gating modes and will be discussed below.

Kinetics of DHS-I-induced Gating Modes

We analyzed durations of normal and drug-modified modes of channel gating to evaluate the relation between DHS-I binding to the channel and modal shifts in channel gating. Durations of normal and drug-modified modes observed in the presence of DHS-I were calculated using criteria described above and plotted in Fig. 9. Mean durations of normal modes decreased from 4.82 to 2.52 s when DHS-I concentration was raised from 33 to 67 nM. According to the framework described above, these durations could reflect the inverse rate of binding of one DHS-I molecule to the channel. The distributions of normal mode durations were well-described by a single exponential component in both 33 and 67 nM DHS-I, as expected for a mechanism where binding of a single DHS-I molecule causes modified gating. Durations of modified modes increased from 2.22 s in 33 nM to 5.41 s in 67 nM DHS-I. Modified durations could reflect mean occupancy times for up to four DHS-I molecules. Distributions of modified modes were best described by two exponential components in both 33 and 67 nM DHS-I. The most significant changes in the distributions of modified modes as DHS-I concentration was raised was an increase in the time constant of the long lifetime component from 8.45 to 12.5 s and an increase in the area of this component from 0.205 to 0.400. When modified mode durations were fit with two exponential components compared with one component, the log likelihoods increased by 130.5 at 33 nM and 46.6 at 67 nM. These improvements in likelihood are highly significant, suggesting that the second component reflects a kinetic process and does not result from stochastic variation. Binding of each DHS-I molecule would create an additional kinetic state and possibly an additional kinetic component in the distribution of modified mode durations, so this data provides evidence for binding of two or more DHS-I molecules to the channel. These kinetic data are consistent with the proposal that normal mode activity represents periods where DHS-I is not bound, and modified modes result from binding of one or more DHS-I molecules.

A similar analysis was performed on three additional single channel experiments (Table I). In three of four experiments analyzed, normal mode durations declined nearly linearly and modified mode durations increased with increasing DHS-I concentration. In the fourth experiment, the normal mode durations declined more steeply with increasing DHS-I concentrations, and modified mode durations were similar at two different DHS-I concentrations. In all these experiments, durations of modified modes were best described by two or more exponential components. Normal mode durations were best described by one or two components, suggesting that, under some conditions, the transition from normal to modified gating requires binding of two DHS-I molecules. In all four experiments, channel open probabilities in the absence of DHS-I were low (0.039–0.13) and, in each case, the probability of occupying the drug-modified mode was typically similar to the average channel open probability in the presence of DHS-I. Thus, the overall increases in channel open probability caused by DHS-I were explained by entry into drug-modified modes of gating.

Kinetic Models for DHS-I-induced Modal Gating

These kinetic data are in harmony with the proposal that maxi-K channel gating can be modified by binding of more than one DHS-I molecule. The model shown in Scheme I, where DHS-I binds to four identical, noninteracting sites on a maxi-K channel, can be transformed to describe DHS-I-induced modes shown in Figs. 7–9. Since normal gating transitions occur on a

TABLE I

Analysis of Gating Modes Induced by DHS-I for Four Single Channel Experiments

Experiment	[DHS-I]	Open probability	Modified mode duration	Normal mode duration	P(modified)	Number of events
	nM		*s*	*s*		
A	0	0.0393	0.099	281	0.0004	6
	33	0.423	2.22	4.82	0.320	267
	67	0.749	5.41	2.52	0.682	102
B	0	0.0164	—	—	0	0
	25	0.115	0.887	15.7	0.0534	129
	75	0.556	3.36	3.80	0.470	305
C	0	0.135	0.922	126	0.0073	14
	25	0.864	6.99	1.87	0.790	259
	50	0.982	53.6	1.03	0.981	31
D	0	0.0488	0.141	273	0.0005	8
	33	0.106	0.469	8.03	0.0552	241
	100	0.288	0.479	1.20	0.285	1983

Modified modes were separated from normal modes in the same manner as was described for experiment A in the text. Average normal and modified mode durations were calculated as described in the METHODS. P(modified) represents the probability of occupancy of a DHS-I-modified mode. Conditions for experiment A were 5 μM calcium, −20 mV, five events were averaged, and events were classified as modified if the mean open time was >200 ms or mean shut time was <10 ms. Conditions for experiment B were 5 μM calcium, −30 mV, and the analysis criteria were the same as used for experiment A. Conditions for experiment C were 2 μM calcium, −30 mV, and averages of 10 events with mean open time >80 ms or mean shut time <10 ms were classified as modified. In experiment D, internal calcium was 20 μM, membrane potential was 30 mV, and averages of 10 events with mean open time >20 ms or mean shut time <10 ms were classified as modified.

much faster time scale than DHS-I induced shifts in channel gating, the closed and open states for each increment of bound DHS-I would be at equilibrium relative to DHS-I binding, except at very low channel open probability. As a result, these sets of states can be combined onto a set of DHS-I gating modes, as shown in Scheme II.

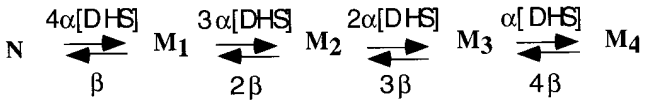

(SCHEME II)

N represents normal mode gating and M1–M4 represent gating modes that occur when one to four DHS-I molecules are bound to the channel, and α and β represent the forward and reverse binding rates, respectively, for DHS-I binding to a single site. This model specifies that binding of a single DHS-I molecule leads to modified gating.

Scheme II allows us to test whether the model of four identical, noninteracting DHS-I binding sites on the maxi-K channel can also describe the kinetics of DHS-I binding. Distributions of normal and modified mode intervals predicted by Scheme II were calculated using Q-matrix methods, as described previously (Colquhoun and Hawkes, 1977, 1981; McManus and Magleby, 1991), and compared with the observed distributions shown in Fig. 9. Optimization of α ($1.7 \times \mu M^{-1}\ s^{-1}$) and β ($0.40\ s^{-1}$) yielded the dotted lines shown in Fig. 9. Distributions of normal mode intervals were accurately described by this model, but distributions of modified modes were poorly fit by this model. These rate constants predict a DHS-I dissociation constant of 240 nM at each site, which is higher than the values estimated for DHS-I binding to closed (130 nM) or open (11 nM) channels based on fitting Scheme I to DHS-I-induced changes in voltage-dependent channel gating.

It is not surprising that Scheme II cannot fully account for the kinetics of DHS-I-induced modal gating. In Scheme II, binding of DHS-I to open and closed states is similar. However, the effects of DHS-I on open probability and voltage-dependent gating require, with thermodynamic certainty, that DHS-I binds with higher affinity to the open versus the closed states. We incorporated this important functional distinction into Scheme III, where f_c and f_o represent forward binding rates to closed and open channels, and b_c and b_o are unbinding rates for closed and open channels, respectively. In this model, we assume that the channel is predominantly closed during normal mode activity and open during modified mode activity. Under these experimental conditions, this approximation is reasonable; channel open probability during normal mode periods was <0.25, but >0.95 during modified mode activity. We optimized these four rates using maximum likelihood fitting of the model to distributions of normal and modified mode durations at two DHS-I concentrations. Predictions of this model using the most likely values of f_c ($1.54\ \mu M^{-1}\ s^{-1}$), b_c ($1.28\ s^{-1}$), f_o ($3.35\ \mu M^{-1}\ s^{-1}$) and b_o ($0.145\ s^{-1}$) are shown as dashed lines

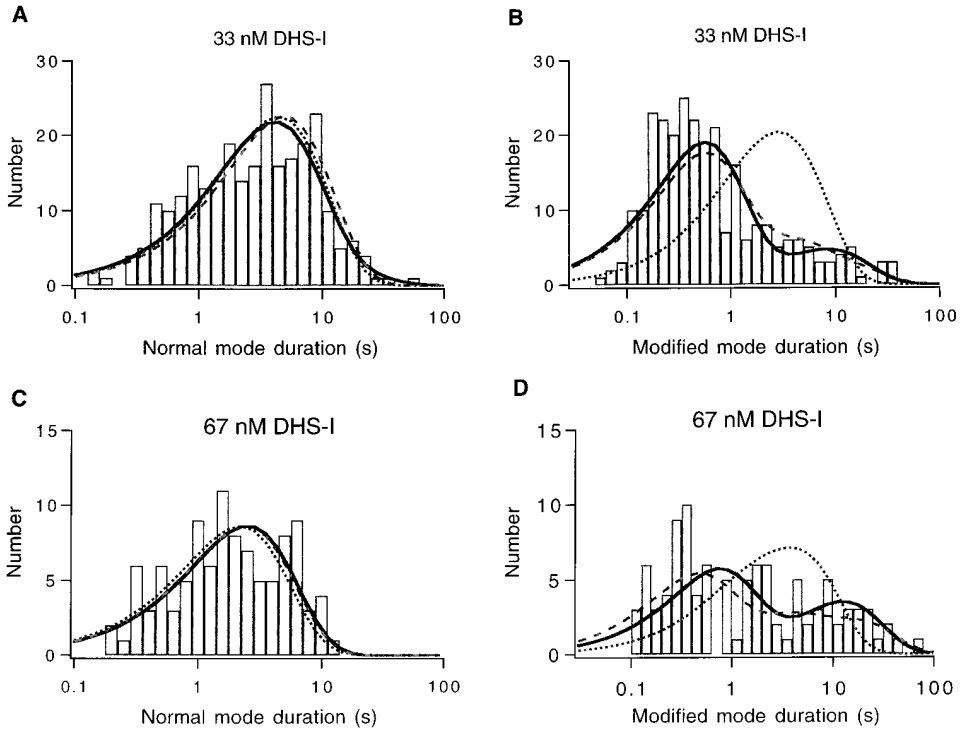

FIGURE 9. Distributions of normal and modified mode durations were calculated from the data shown in Figs. 7 and 8 using criteria described in the text and binned logarithmically. Solid lines represent maximum likelihood fits to the distributions with one exponential component for the normal mode distributions and two exponential components for the modified mode distributions. The dotted lines represent predictions of a four-independent, noninteracting site model (Scheme II) and the dashed lines represent the predictions of Scheme III that allows different binding affinities to open and closed states.

in Fig. 9, and provide an excellent description of the data. Using these rate constants, we calculate a microscopic binding constant of 830 nM to closed channels and 43 nM to open channels. The results of this kinetic analysis are in harmony with analysis of equilibrium effects of DHS-I on voltage-dependent channel gating. We find that DHS-I binds more tightly (19-fold) to open compared with closed channels, and that a simple model with four identical, noninteracting DHS-I binding sites can explain the data.

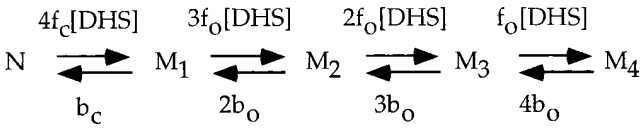

(SCHEME III)

Do the simplifying assumptions used above limit the ability of these kinetic schemes to describe the data? To examine this possibility, we relaxed the restriction in Schemes II and III prohibiting interactions between binding sites, and allowed the eight rate constants in Scheme IV to vary independently. We fit this model, shown in Scheme IV, to distributions of normal and modified periods at two DHS-I concentrations using maximum likelihood and Q-matrix methods. The predictions of Scheme IV give a good description of the data (not shown) and nearly overlaid the predictions of Scheme III. Forward rates for DHS-I binding to the first (R_1), second (R_2), and third (R_3) sites were 6.15, 13.5, and 2.12 μM^{-1} s^{-1}, respectively. Unbinding rates for the first through third sites were 1.39, 0.312, and 0.136 s^{-1}, respectively. Rates R_4 and R_{-4} were not adequately determined and could be changed several fold with little effect on the overall likelihood. In fact, removing state M_4 did not affect the maximum likelihood of the model after reoptimization (not shown). The model contains eight parameters and the four distributions obtained at two DHS-I concentrations specify eight parameters, with some redundancy. Thus, it is not surprising that rates furthest removed from the gateway between normal and modified modes are poorly determined.

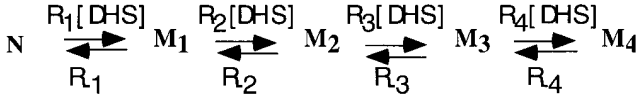

(SCHEME IV)

Scheme III describes distributions of normal and modified periods in Fig. 9 nearly as well as Scheme IV, which has four additional free parameters. The log likelihood ratio obtained by comparing the likelihood of Scheme IV with the likelihood of Scheme III was 2.3, which is not a significant improvement (likelihood ratio test [Rao, 1973; Horn and Lange, 1983] with four degrees of freedom at $P < 0.05$ level). A simplified version of Scheme IV described above lacks state M_4 and has six free parameters, but did not fit the distributions significantly better than Scheme III with four free pa-

rameters (likelihood ratio test with two degrees of freedom at $P < 0.05$ level). Thus, Scheme III is the most economical model considered that adequately describes the data. This implies that the assumptions of four independent sites and differential binding to open versus closed states incorporated in Scheme III are consistent with the data.

Inspection of the rate constants obtained for Scheme IV, where all rates are independent, lends further support for Scheme III. The rate constants in Scheme IV can be used to estimate microscopic binding constants to individual sites. If we assume that the channel contains four identical sites and that DHS-I binding can occur in any order, then the microscopic K_ds for binding of the first through third DHS-I molecules were 900, 35, and 43 nM, respectively. A >20-fold increase in binding affinity occurred after binding of the first DHS-I molecule. These microscopic K_ds nearly match the binding constants estimated for closed (830 nM) and open (43 nM) channels with Scheme III.

A kinetic analysis of DHS-I interaction with single maxi-K channels revealed periods of high channel open probability that may be associated with binding of DHS-I. The results of this kinetic analysis are in agreement with a picture derived from analysis of equilibrium effects of DHS-I on channel open probability and voltage-dependent channel opening. DHS-I can bind to four or more functional sites on each maxi-K channel and can promote channel opening by binding with 10–20-fold higher affinity to open states compared with closed states. Further, the kinetics of binding obtained from this analysis suggest this increase in affinity primarily comes from a slower dissociation rate for the open state.

DISCUSSION

DHS-I Activates Maxi-K Channels through a High-Order Binding Reaction

Three separate lines of evidence suggest multiple sites on maxi-K channels for activation by DHS-I. First, the relationship between open probability and DHS-I concentration was well described by a Hill equation with an average slope (N_{DHS-I}) of 2.4, which suggests that three or more DHS-I molecules must bind to maximally activate the maxi-K channel. Second, the shift in voltage-dependent channel opening caused by DHS-I was quantitatively described (Fig. 5 *D*) by a simple model (Scheme I) that specified four functional binding sites for DHS-I on each maxi-K channel. A similar model with only one DHS-I binding site was clearly inadequate.

The third line of evidence supporting a multi-site model for channel activation by DHS-I comes from kinetic analysis of channel gating. Examination of single channel data recorded in the presence of DHS-I revealed periods of high open probability interleaved with periods of lower open probability resembling control gating. A simple explanation of these drug-induced gating transitions is that they reflect binding and unbinding of DHS-I from the channel. A kinetic analysis of these DHS-I-induced gating modes revealed the durations of the drug-modified periods increased with drug concentration, suggesting that more than one DHS-I molecule could bind to the channel at once. The distributions of drug-modified modes were best fit by two or more exponential components for each experimental condition ($n = 8$), further supporting a multi-site model for DHS-I binding.

DHS-I Differentially Modifies Calcium- and Voltage-dependent Gating

The gating of maxi-K channels is dually regulated by both calcium and membrane potential. The question naturally arises, whether calcium and voltage regulate channel opening by the same or separate mechanisms. An early model proposed that channels opened in response to calcium, and that membrane potential regulated binding of calcium to sites located within the membrane field (Moczydlowski and Latorre, 1983). In this case, calcium and voltage act through a single mechanism. More recent work provides evidence that calcium and voltage regulate channel opening via separate, but linked, mechanisms (DiChiara and Reinhart, 1995; Cox et al., 1997; Cui et al., 1997; Stefani et al., 1997).

DHS-I shifted both calcium- and voltage-dependent activation curves. We now examine specific effects of DHS-I on calcium- and voltage-dependent activation properties with the aim of resolving differences in activation by either stimulus. The answer could be used to predict the effects of this compound on channel activity in a physiological context, and may reveal aspects of the linkage between calcium- and voltage-dependent channel activation.

The relationships between open probability and calcium and membrane potential describe how these two stimuli modulate the equilibrium for channel opening. It follows that the K_{Ca} and $V_{1/2}$ values derived from these relationships are both related to the equilibrium for channel opening. A threefold decrease in K_{Ca} was caused by 100 nM DHS-I. Using the Hill equation for calcium (Fig. 4) and a slope of two to three, this corresponds to an ~10–30-fold increase in the equilibrium for channel opening. In contrast, 100 nM DHS-I caused an 80-mV shift in $V_{1/2}$. Using the Boltzmann equation (Eq. 5) and a slope (s) value of 11.5 mV, this shift corresponds to an ~1,000-fold increase in the equilibrium for channel opening. This suggests that DHS-I differentially modulates calcium- versus voltage-dependent gating. These differential effects of DHS-I can be evalu-

ated in another way. Analysis of maxi-K channel currents from heterologously expressed α and β subunits showed that a threefold change in calcium over the range of 1–100 μM results in a 30–50-mV shift in the midpoint for voltage-dependent activation (McManus et al., 1995; Dworetzky et al., 1996; Meera et al., 1996). These shifts in $V_{1/2}$ caused by calcium are less than the shift in $V_{1/2}$ caused by DHS-I in our present experiments. Together, these findings suggest that DHS-I differentially modulates voltage- versus calcium-dependent channel gating, with larger shifts occurring for voltage-dependent gating than for calcium-dependent gating. These differences in effects of DHS-I on calcium- and voltage-dependent gating suggest that calcium- and voltage-dependent gating mechanisms are not the same and that calcium and voltage modify the equilibrium for channel opening through discrete processes.

Our data suggest that DHS-I may independently modify voltage-dependent gating. If true, then we would expect DHS-I to shift voltage-dependent gating in the virtual absence of calcium. Previously, we showed that DHS-I could not activate the channel in the virtual absence of calcium at membrane potentials $<+40$ mV (McManus et al., 1993*b*). However, under these conditions, the shift in equilibrium for channel opening caused by DHS-I might not be sufficient to cause channel opening in the absence of calcium. Alternatively, binding of at least one calcium ion may be necessary for DHS-I binding or efficacy. These distinctions can be more fully characterized in heterologous expression systems where a wider range of membrane voltage can be explored.

A Simple Four-Site Model Describes Changes in Voltage-dependent Gating

The effects of DHS-I on voltage-dependent gating can be described by a model where DHS-I binding increases the equilibrium for channel opening, K_{eq}. For simplicity, we propose that, in the absence of DHS-I, the channel equilibrates between two sets of conformational states, closed and open, and the equilibrium between these states is voltage dependent. DHS-I increases the equilibrium by binding more tightly to the open, potassium permeant, conformation. At least three to four DHS-I molecules may be required to maximally activate the channel. Since maxi-K channels are likely composed of four α (Shen et al., 1994) and four β (Garcia-Calvo et al., 1994; Giangiacomo et al., 1995) subunits, we proposed that there are four identical, noninteracting DHS-I sites (see Scheme I).

This model specifies a two-state mechanism for channel gating in the absence of DHS-I, which is a gross simplification compared with recent models used to describe maxi-K channel gating (McManus and Magleby, 1991; Cox et al., 1997). The assumption behind this simplification is that a single rate-limiting, voltage-dependent step divides families of closed from families of open states. This assumption is supported by recent analysis of voltage activation of cloned maxi-K channel α subunits (Cox et al., 1997; Cui et al., 1997). Analysis of single channel kinetics of skeletal muscle maxi-K channels showed that at least five closed and three open states are needed to account for calcium-dependent changes in channel gating (McManus and Magleby, 1991). Statistical analysis of the sequence of occurrence of open and closed events demonstrated multiple transition pathways that connect these open and closed states (McManus et al., 1985). Despite these complexities, models that best describe the calcium-dependent gating of skeletal muscle maxi-K channels predict that the majority of the transitions between open and closed states follow one pathway (McManus and Magleby, 1991). We admit that the two-state model is clearly an oversimplification of channel gating in the absence of DHS-I, but propose that it can serve as a useful starting point for analysis of modification of voltage-dependent gating by DHS-I.

To test this model, we derived an expression (Eq. 7) that relates the shift in voltage-dependent gating caused by DHS-I to the high order binding of DHS-I to closed and open channel conformations (shown in Scheme I). This expression includes the number of DHS-I binding sites and the microscopic equilibrium dissociation constants for closed (k_c) and open (k_o) states of the channel. The observed shift in $V_{1/2}$ caused by DHS-I was well described by this simple four-site model with a 12-fold enhanced affinity for binding to the open state compared with the closed state. The maximum amplitude of this hyperpolarizing shift, ~100 mV, reflects the maximum increase in channel opening that can be obtained from the binding four DHS-I molecules.

The increase in equilibrium for channel opening, K_{eq}, caused by DHS-I is predicted to be finite and saturable. In contrast, membrane potential can either increase or decrease the equilibrium for channel opening. At very negative potentials, the open probability, and hence K_{eq}, in the absence of DHS-I can become very small. Thus, when the increase in K_{eq} caused by DHS-I is equal and opposite that caused by membrane potential, then P_o should saturate at values close to 0.5. Fitting this model (Scheme I) to the relation between $\Delta V_{1/2}$ and concentration of DHS-I (Fig. 5 *D*) led to the prediction that at -70 mV the opposing effects of membrane potential and DHS-I on K_{eq} should be equally balanced. These predictions closely matched the effects of saturating amounts of DHS-I on open probability (Fig. 6). Thus, this model has predictive as well as descriptive power.

Comparing Equilibrium and Kinetic Effects of DHS-I

We examined the equilibrium and kinetic effects of DHS-I on channel gating. Both types of analysis revealed the presence of multiple DHS-I binding sites on maxi-K channels with 10–20-fold tighter binding to open versus closed channels. However, these two types of experiments were done under different conditions, consequently some differences are expected. The kinetic experiments suggest that binding of one or two DHS-I molecules can cause an observable shift in channel gating, increasing channel open probability from low (0.01—0.1) to high (>0.9) values. However, equilibrium measurements of open probability versus DHS-I concentration yielded Hill slopes for DHS-I of two to three. This suggests that binding of three or more DHS-I molecules was necessary to achieve maximal channel open probability under these conditions. These differences result from the lower control channel open probabilities in the equilibrium measurements, where binding of multiple DHS-I molecules is necessary to fully activate the channel.

These considerations predict that, when control open probability is very low, binding of a single DHS-I molecule should cause the appearance of modified modes where the open probability is $<<1$. Consequently, different modes corresponding to various numbers of bound DHS-I molecules might be detectable. However, under these conditions, channel openings are infrequent and averaged closed times are long. Hence, it becomes difficult to resolve gating changes lasting only a few seconds. Careful titration of control channel open probability may allow resolution of different gating modes.

Mechanistic Implications from DHS-I Binding Kinetics

Analysis of the kinetics of DHS-I modification of maxi-K channel gating provides a way to further examine the mechanism of DHS-I action. A statistical analysis of channel gating in the presence of DHS-I revealed two discrete modes of channel gating. We proposed that one mode represents periods of drug-modified gating, and the other mode represents periods of normal gating. We performed a kinetic analysis of these periods of normal and drug-modified modes and were able to describe these kinetic data with a simple model, which specified four identical, noninteracting DHS-I binding sites and allowed different binding affinities for open and closed states (Scheme III). The most likely rate constants for this model predicted a 19-fold enhanced affinity for DHS-I binding to open versus closed channel states. This four parameter model described the kinetic data as well as a more general model containing more free parameters that allowed interactions between binding sites.

The effects of DHS-I on channel gating and our kinetic model for DHS-I action (Scheme III) suggest a physical mechanism for DHS-I action. Our analysis of normal modes observed in the presence of DHS-I suggests that binding of one DHS-I molecule was sufficient to induce a DHS-I modified mode. In addition, there are at least two modified modes that likely reflect different levels of occupancy by DHS-I. From low open probability, binding of the first DHS-I molecule most likely occurs through the closed conformation of the channel. This results from equilibrium considerations because the channel is closed most of the time. Binding of subsequent DHS-I molecules most likely occurred through open channels in these experiments, since the open probability of modified periods was >0.95. Fitting normal and modified mode durations (Fig. 9) to a kinetic model (Scheme III) allowed estimation of the microscopic rates of DHS-I binding to open and closed channels. The association rate of DHS-I was twofold higher for open compared with closed channels. This suggests that the DHS-I binding site is similarly accessible in both open and closed conformations. The DHS-I dissociation rate was ninefold slower from open channels versus closed channels. It is unlikely that a conformational change associated with opening prevents egress of DHS-I since the DHS-I association rate is increased for open channels. Thus, the increase in equilibrium for channel opening caused by DHS-I most likely derives from its thermodynamically more favorable interaction with open channels.

Binding Sites for DHS-I

What can electrophysiological experiments tell us about the binding sites for DHS-I on maxi-K channels? First, the present experiments suggest that each maxi-K channel contains at least four DHS-I binding sites, which agrees with the expected stoichiometry of this channel (Garcia-Calvo et al., 1994; Shen et al., 1994). Lipid bilayer experiments have shown that these binding sites are only accessible to DHS-I from the cytoplasmic side (McManus et al., 1993*b*). Coexpression experiments have shown that the β subunit confers sensitivity to DHS-I, as channels composed of only α subunits are DHS-I insensitive (McManus et al., 1995). This finding implies that DHS-I binding sites are associated with, or allosterically coupled to, β subunits. By comparison, calcium-dependent activation of α subunits is also modified by presence of β subunits (McCobb et al., 1995; McManus et al., 1995; Wallner et al., 1995; Dworetzky et al., 1996; Tseng-Crank et al., 1996), and calcium binding sites are contained on the α subunit. We observed variability in the sensitivity of DHS-I to channel gating reflected in measured K_{DHS} values (Fig. 3). The essential role of the β subunit in conferring DHS-I sensitivity

and its modulatory role on calcium-sensitive gating may underlie some of this observed variability.

Mapping experiments suggest that the β subunit is composed of two transmembrane domains, a long extracellular loop, and two short intracellular segments (Knaus et al., 1994), leaving little to construct an intracellular binding site for DHS-I. By default, DHS-I binding sites may be located on α subunits or on transmembrane segments of the β subunits. In either case, the conformation of the binding site is altered during channel gating, as DHS-I stabilizes channel open states. The binding site appears to be unique to maxi-K channels as small-conductance, calcium-activated potassium channels in T-lymphocytes and a variety of other ion channels are not affected by DHS-I (McManus et al., 1993*b*).

Chemical modifications of DHS-I at either end of the molecule can cause substantial changes in activity, suggesting that the DHS-I binding site may be nearly as large as the entire DHS-I molecule (McManus et al., 1993*b*). The triterpene portion is likely to be rigid and hydrophobic, with dimensions of $\sim 14 \times 5.5 \times 4$ Å, and may bind to a hydrophobic site. The first two sugar residues attached to the triterpene are required for full activity, but probably do not bind to a site located within the membrane field. This is based on our finding that changes in membrane potential over a 60-mV range did not affect DHS-I binding (Fig. 3). This implies that if DHS-I binding sites are aligned orthogonal to the plane of the membrane, then the hydrophilic sugar residues would face the cytoplasmic side.

DHS-I clearly binds to sites that are important for maxi-K channel gating. The precise location of DHS-I binding sites on the maxi-K channel may help elucidate the structural and functional relationships that underlie maxi-K channel gating.

We thank Dr. Marion Addy for supplying samples of *Desmodium adscendens* and Dr. Karl Magleby for comments on the manuscript.

Original version received 1 June 1998 and accepted version received 10 August 1998.

REFERENCES

Colquhoun, D., and A.G. Hawkes. 1977. Relaxation and fluctuations of membrane currents that flow through drug operated channels. *Proc. R. Soc. Lond. B Biol. Sci.* 199:231–262.

Colquhoun, D., and A.G. Hawkes. 1981. On the stochastic properties of single ion channels. *Proc. R. Soc. Lond. B Biol. Sci.* 211:205–235.

Cox, D.H., J. Cui, and R.W. Aldrich. 1997. Allosteric gating of a large conductance Ca-activated K^+ channel. *J. Gen. Physiol.* 110: 257–281.

Cui, J., D.H. Cox, and R.W. Aldrich. 1997. Intrinsic voltage dependence and Ca^{2+} regulation of *mslo* large conductance Ca-activated K^+ channels. *J. Gen. Physiol.* 109:647–673.

DiChiara, T.J., and P.H. Reinhart. 1995. Distinct effects of Ca^{2+} and voltage on the activation and deactivation of cloned Ca^{2+}-activated K^+ channels. *J. Physiol. (Camb.).* 489:403–418.

Dworetzky, S.I., C.G. Boissard, J.T. Lum-Ragan, M.C. McKay, D.J. Post-Munson, J.T. Trojnacki, C.-P. Chang, and V.K. Gribkoff. 1996. Phenotypic alteration of a human BK (*hslo*) channel by *hslo*β subunit coexpression: changes in blocker sensitivity, activation/relaxation and inactivation kinetics, and protein kinase A modulation. *J. Neurosci.* 16:4543–4550.

Galvez, A., G. Gimenez-Gallego, J.P. Reuben, L. Roy-Contancin, P. Feigenbaum, G.J. Kaczorowski, and M.L. Garcia. 1990. Purification and characterization of a unique, potent, peptidyl probe for the high conductance calcium-activated potassium channel from venom of the scorpion Buthus tamulus. *J. Biol. Chem.* 265:11083–11090.

Garcia-Calvo, M., H.-G. Knaus, O.B. McManus, K.M. Giangiacomo, G.J. Kaczorowski, and M.L. Garcia. 1994. Purification and reconstitution of the high-conductance, calcium-activated potassium channel from tracheal smooth muscle. *J. Biol. Chem.* 269:676–682.

Giangiacomo, K.M., M.L. Garcia, and O.B. McManus. 1992. Mechanism of Iberiotoxin block of the large-conductance calcium-activated potassium channel from bovine aortic smooth muscle. *Biochemistry.* 31:6719–6727.

Giangiacomo, K.M., M. Garcia-Calvo, H.-G. Knaus, T.J. Mullmann, M.L. Garcia, and O.B. McManus. 1995. Functional reconstitution of the large-conductance, calcium-activated potassium channel purified from bovine aortic smooth muscle. *Biochemistry.* 34: 15849–15862.

Hess, P., J.B. Lansman, and R.W. Tsien. 1984. Different modes of Ca channel gating behaviour favoured by dihydropyridine Ca agonists and antagonists. *Nature.* 311:538–544.

Horn, R., and K. Lange. 1983. Estimating kinetic constants from single channel data. *Biophys. J.* 43:207–223.

Hu, S., C.A. Fink, H.S. Kim, and R.W. Lappe. 1997. Novel and potent BK channel openers: CGS 7181 and its analogues. *Drug Dev. Res.* 41:10–21.

Knaus, H.-G., A. Eberhart, G.J. Kaczorowski, and M.L. Garcia. 1994. Covalent attachment of charybdotoxin to the β-subunit of the high-conductance Ca^{2+}-activated K^+ channel. *J. Biol. Chem.* 269: 23336–23341.

Latorre, R., C. Vergara, and C. Hidalgo. 1982. Reconstitution in planar lipid bilayers of a Ca^{2+}-dependent K^+ channel from transverse tubule membranes isolated from rabbit skeletal muscle. *Proc. Natl. Acad. Sci. USA.* 79:805–809.

MacKinnon, R., and C. Miller. 1988. Mechanism of charybdotoxin block of the high-conductance, Ca^{2+}-activated K^+ channel. *J. Gen. Physiol.* 91:335–349.

MacKinnon, R., and C. Miller. 1989. Functional modification of a Ca^{2+}-activated K^+ channel by trimethyloxonium. *Biochemistry.* 28: 8087–8092.

Marty, A. 1981. Ca-dependent K channels with large unitary conductance in chromaffin cell membranes. *Nature.* 291:497–500.

McCobb, D.P., N.L. Fowler, T. Featherstone, C.J. Lingle, M. Saito,

J.E. Krause, and L. Salkoff. 1995. A human calcium-activated potassium channel gene expressed in vascular smooth muscle. *Am. J. Physiol.* 269:H767–H777.

McManus, O.B., A.L. Blatz, and K.L. Magleby. 1985. Inverse relationship of the durations of adjacent open and shut intervals for Cl and K channels. *Nature.* 317:625–627.

McManus, O.B., A.L. Blatz, and K.L. Magleby. 1987. Sampling, log binning, fitting and plotting durations of open and shut intervals from single channels and the effects of noise. *Pflügers Arch.* 410: 530–553.

McManus, O.B., K.L. Giangiacomo, G.H. Harris, M.E. Addy, J.P. Reuben, G.J. Kaczorowski, and M.L. Garcia. 1993*a*. A maxi-K channel agonist isolated from a medicinal herb. *Biophys. J.* 64:3*a*. (Abstr.)

McManus, O.B., G.H. Harris, K.M. Giangiacomo, P. Feigenbaum, J.P. Reuben, M.E. Addy, J.F. Burka, G.J. Kaczorowski, and M.L. Garcia. 1993*b*. An activator of calcium-dependent potassium channels isolated from a medicinal herb. *Biochemistry.* 32:6128–6133.

McManus, O.B., L.M.H. Helms, L. Pallanck, B. Ganetzky, R. Swanson, and R.J. Leonard. 1995. Functional role of the β subunit of high conductance calcium-activated potassium channels. *Neuron.* 14:645–650.

McManus, O.B., and K.L. Magleby. 1991. Accounting for the Ca^{2+}-dependent kinetics of single large-conductance Ca^{2+}-activated K^+ channels in rat skeletal muscle. *J. Physiol. (Camb.).* 443:739–777.

Meera, P., M. Wallner, Z. Jiang, and L. Toro. 1996. A calcium switch for the functional coupling between α (*hslo*) and β subunits ($K_{V,Ca\beta}$) of maxi-K channels. *FEBS Lett.* 382:84–88.

Miller, C., E. Moczydlowski, R. Latorre, and M. Phillips. 1985. Charybdotoxin, a protein inhibitor of single Ca^{2+}-activated K^+ channels from mammalian skeletal muscle. *Nature.* 313:316–318.

Moczydlowski, E., and R. Latorre. 1983. Gating kinetics of Ca^{2+}-activated K^+ channels from rat muscle incorporated into planar lipid bilayers: evidence for two voltage-dependent Ca^{2+} binding reactions. *J. Gen. Physiol.* 82:511–542.

Moczydlowski, E., K. Lucchesi, and A. Ravindran. 1988. An emerging pharmacology of peptide toxins targeted against potassium channels. *J. Membr. Biol.* 105:95–111.

Olesen, S.P., E. Munch, F. Watjen, and F. Drejer. 1994. Selective activation of Ca^{2+}-dependent K^+ channels by novel benzimidazolone. *Eur. J. Pharmacol.* 251:53–59.

Pallotta, B.S., K.L. Magleby, and J.N. Barrett. 1981. Single channel recordings of Ca^{2+}-activated K^+ currents in rat muscle cell culture. *Nature.* 293:471–474.

Park, C.-S., and C. Miller. 1992*a*. Interaction of charybdotoxin with permeant ions inside the pore of a K^+ channel. *Neuron.* 9:307–313.

Park, C.-S., and C. Miller. 1992*b*. Mapping function to structure in a channel-blocking peptide: electrostatic mutants of charybdotoxin. *Biochemistry.* 31:7749–7755.

Rao, C.R. 1973. Linear Statistical Inference and Its Applications. John Wiley, New York.

Shen, K.Z., A. Lagrutta, N.W. Davies, N.B. Standen, J.P. Adelman, and R.A. North. 1994. Tetraethylammonium block of Slowpoke calcium-activated potassium channels expressed in *Xenopus* oocytes: evidence for tetrameric channel formation. *Pflügers Arch.* 426:440–445.

Singh, S.B., M.A. Goetz, D.L. Zink, A.W. Dombrowski, J.D. Polishook, M.L. Garcia, W. Schmalhofer, O.B. McManus, and G.J. Kaczorowski. 1994. Maxikdiol: a novel dihydroxyisoprimane as an agonist of maxi-K channels. *J. Chem. Soc. Perkin Trans. I.* 1:3349–3352.

Slaughter, R.S., J.L. Shevell, J.P. Felix, M.L. Garcia, and G.J. Kaczorowski. 1989. High levels of sodium-calcium exchange in vascular smooth muscle sarcolemmal membrane vesicles. *Biochemistry.* 28: 3995–4002.

Stampe, P., L. Kolmakova-Partensky, and C. Miller. 1994. Intimations of K^+ channel structure from a complete functional map of the molecular surface of charybdotoxin. *Biochemistry.* 33:443–450.

Stefani, E., M. Ottolia, F. Noceti, R. Olcese, M. Wallner, R. Latorre, and L. Toro. 1997. Voltage-controlled gating in a large conductance Ca^{2+}-sensitive K^+ channel (*hslo*). *Proc. Natl. Acad. Sci. USA.* 94:5427–5431.

Tseng-Crank, J., N. Godinot, T.E. Johanson, P.K. Ahring, D. Strobaek, R. Mertz, C.D. Foster, S.-P. Olesen, and P.H. Reinhart. 1996. Cloning, expression, and distribution of a Ca^{2+}-activated K^+ channel β-subunit from human brain. *Proc. Natl. Acad. Sci. USA.* 93:9200–9205.

Wallner, M., P. Meera, M. Ottolia, G.J. Kaczorowski, R. Latorre, M.L. Garcia, E. Stefani, and L. Toro. 1995. Characterization of and modulation by a β-subunit of a human Maxi K_{Ca} channel cloned from myometrium. *Receptors Channels.* 3:185–199.